Electronic Supplementary Material (ESI) for Journal of Materials Chemistry C.

Supporting information

Defect-induced broadband photodetection of layered γ-In_2Se_3 nanofilm and its application in near infrared image sensor

Chun-Yan Wu, Jing-Wei Kang, Bin Wang, Hui-Nan Zhu, Zhong-Jun Li, Shi-Rong Chen, Li Wang, Wen-Hua Yang, Chao Xie, Lin-Bao Luo**

School of Electronic Science and Applied Physics, Hefei University of Technology, Hefei, Anhui 230009, China

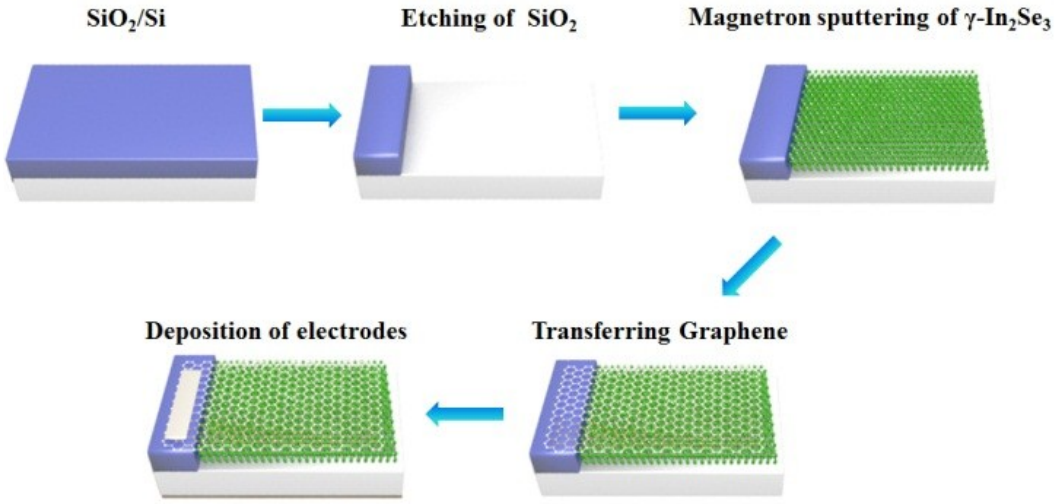

Figure S1. Schematic illustration for the fabrication of γ-In_2Se_3/n-Si heterojunction.

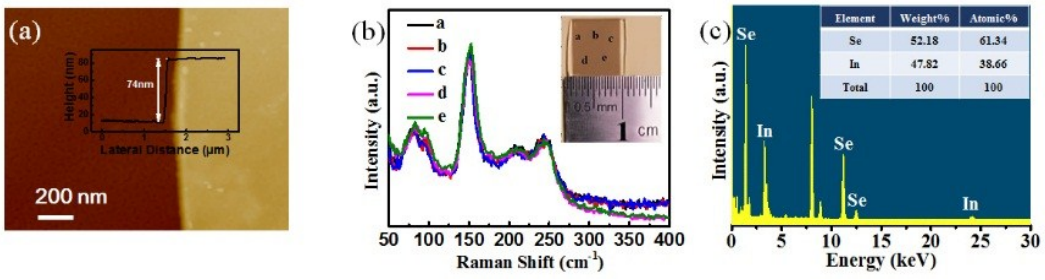

Figure S2. (a) AFM image of the γ-In_2Se_3 nanofilm on SiO_2/Si substrate. Inset shows the height profile. (b) Raman spectra of five random spots on the film surface. Inset shows the photograph of the film. (c) EDS spectrum of In_2Se_3 film. Inset shows the weight and atomic ratios of Se and In elements.

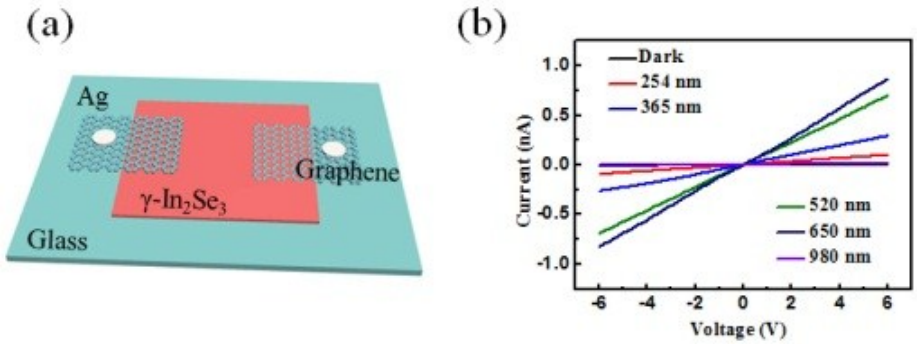

Figure S3. (a) Schematic illustration of the graphene/γ-In_2Se_3/graphene photodetector. (b) $I-V$ curves of In_2Se_3 nanofilm in dark and upon illumination with different wavelength.

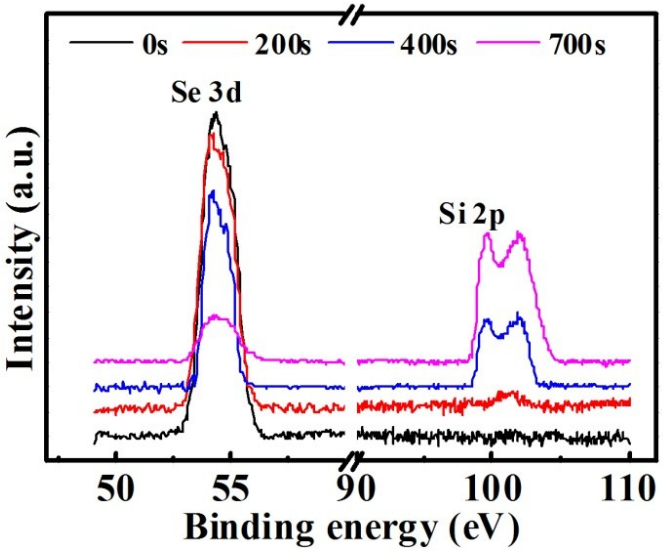

Figure S4. XPS spectra of the γ-In_2Se_3/Si interface obtained after Ar^+ ion sputtering for different time.

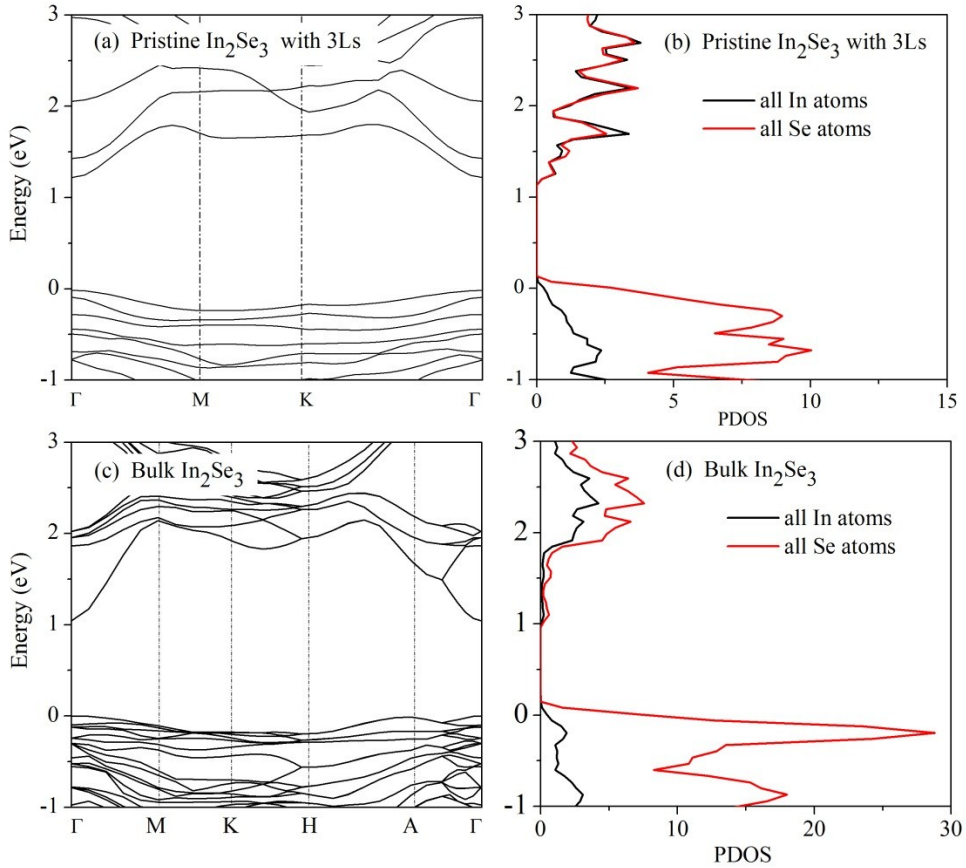

Figure S5. Band structures and PDOS of (a,b) pristine γ-In_2Se_3 with 3Ls and (c,d) the bulk γ-In_2Se_3.

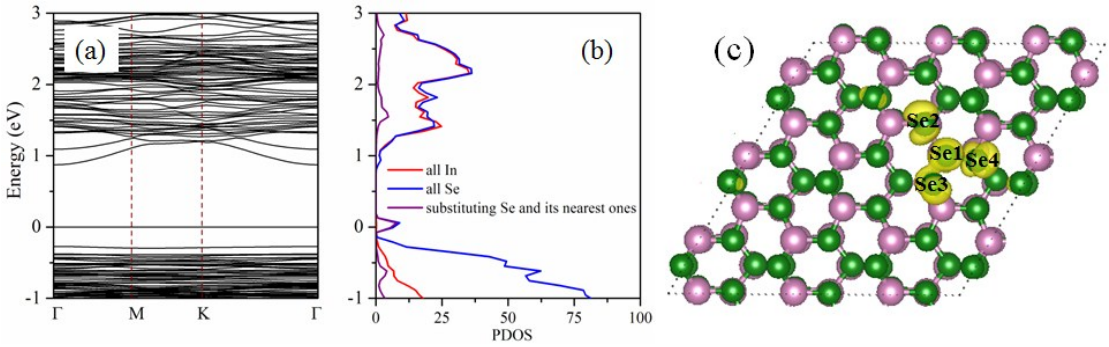

Figure S6. (a) Band structures, (b) PDOS, and (c) electron density distribution of the gap state near Fermi level for Se-substituting In_2Se_3 in a 3×3 supercell. In PDOS, the red, green, and blue lines denote the contribution from all In, all Se, and the substituting Se (Se1) and its three nearest ones (Se2, Se3, and Se4).

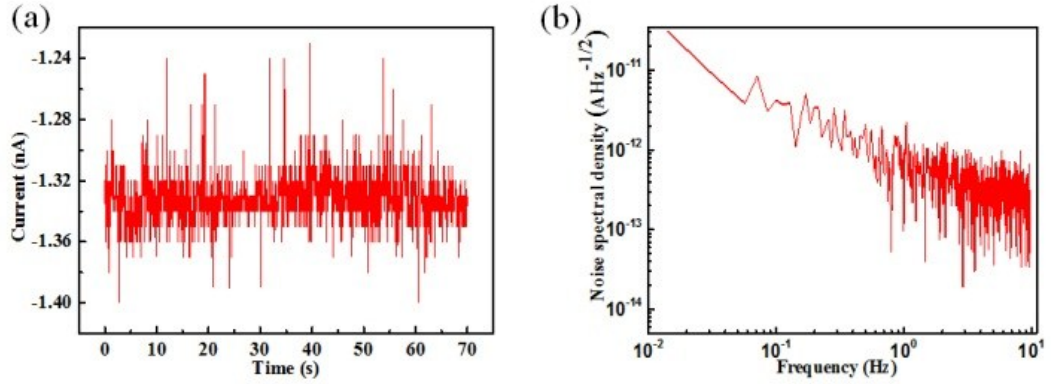

Figure S7. (a) Dark current of the γ-In_2Se_3/Si photodetector under zero bias. (b) The noise spectral density based on the Fourier transform of the dark current.

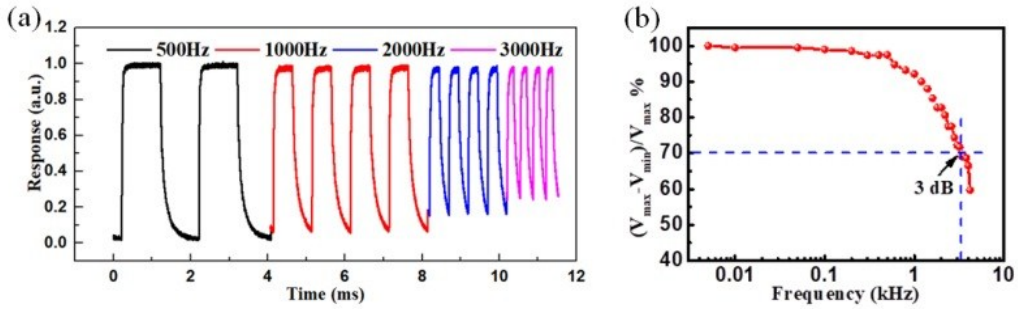

Figure S8. (a) Response of the photodetector to the pulsed radiation at a frequencies of 500, 1000, 2000 and 3000 Hz, respectively. (b) Relative balance $(V_{max}—V_{min})/V_{max}$ versus switching frequency.

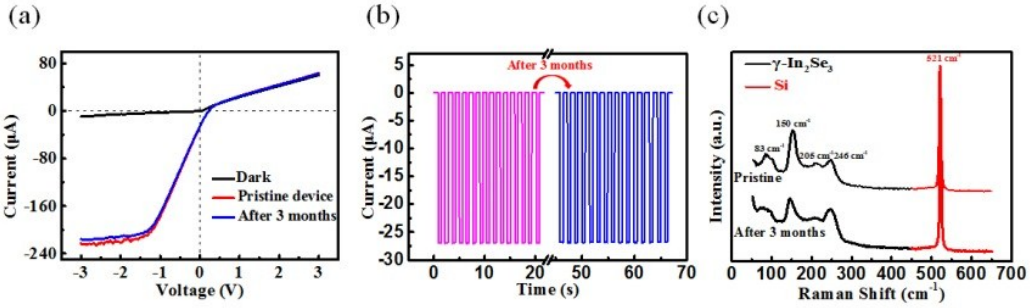

Figure S9. (a) *I–V* characteristics, (b) time-dependent photoresponse at zero bias of the γ-In_2Se_3/*n*-Si photodetector and (c) Raman spectra of the γ-In_2Se_3 film before and after 3 months storage in air.

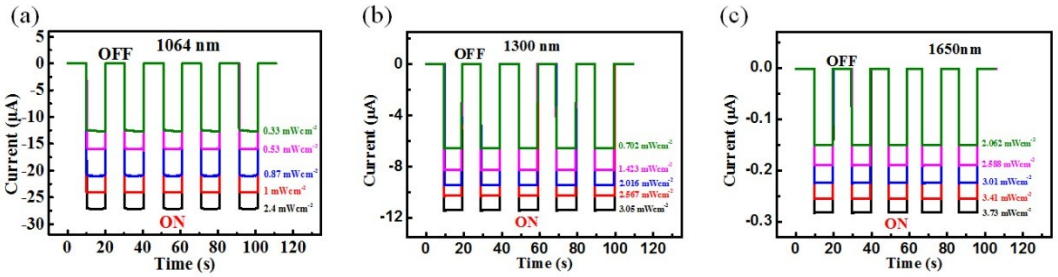

Figure S10. Time-dependent photoresponse of the γ-In_2Se_3/Si photodetector under (a) 1064 nm, (b) 1300 and (c) 1650 nm, respectively.

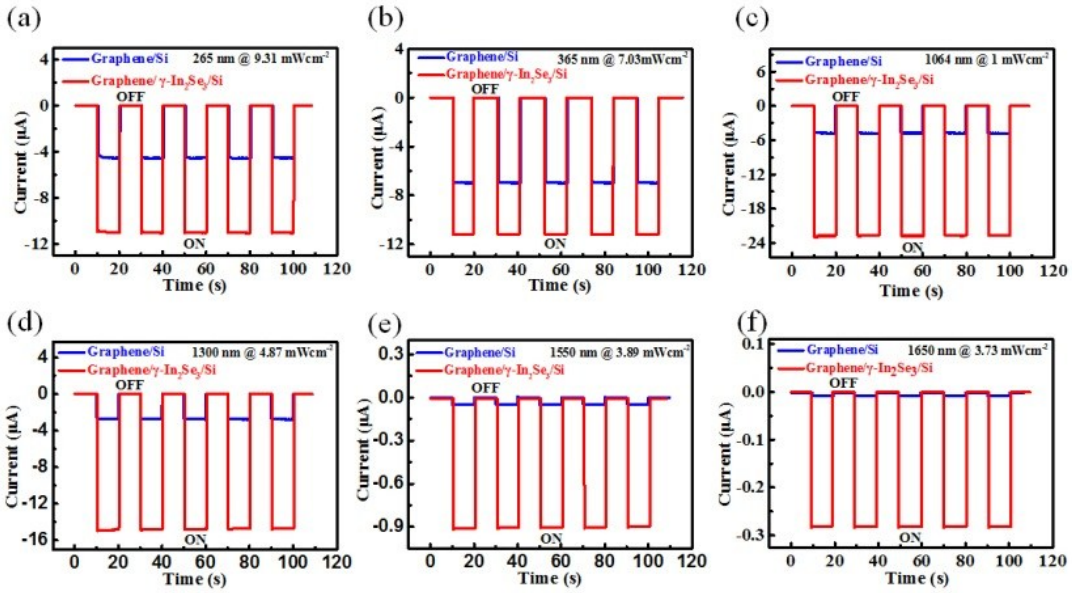

Figure S11. Photocurrent switching performances of graphene/planar Si and graphene/γ-In_2Se_3/planar Si devices measured under different light illumination.